GPS Solut
DOI 10.1007/s10291-013-0353-5

ORIGINAL ARTICLE

Improved detection of earthquake-induced ground motion with spatial filter: case study of the 2012 $M = 7.6$ Costa Rica earthquake

Haitao Yin · Shimon Wdowinski

Received: 6 August 2013 / Accepted: 30 October 2013

Abstract High-rate GPS measurements of earthquake-induced strong crustal movements reveal important information on large amplitude displacements, which cannot be obtained by other seismic monitoring equipment. However, obtaining accurate measurements of these strong movements can be challenging, because large magnitude earthquakes ($M > 7$) affect a wide area surrounding the epicenter. As a result, the GPS recorded movements are calculated with respect to distant sites (relative positioning), or with satellite parameters estimated from distant sites (precise point positioning). In order to improve the accuracy of the strong motion GPS measurements, we developed a new method, based on a spatial filtering technique. The method calculates the displacement of a high-rate monitoring network with respect to a moving near field site and uses a stacking technique to remove the movements of the reference site from all the time series. We applied the new method to the analysis of 5 Hz data acquired by the Nicoya Peninsula network, which recorded strong crustal movements induced by the 2012, $M = 7.6$ Costa Rica earthquake. The results were successfully tested with respect to 1 Hz time series calculated with a far field reference site. The spatial filtering method also removes other systematic common noise from the time series, possibly due to atmospheric delay or orbital errors and, hence, produces more accurate solutions that those based on far fields sites, or on near field site experiencing earthquake-induced action.

Keywords High-rate GPS · Spatial filter · Ground motion · Earthquake

H. Yin (✉)
Earthquake Administration of Shandong Province, Jinan, China
e-mail: yinhaitao121@163.com

H. Yin · S. Wdowinski
Division of Marine Geology and Geophysics, University of Miami, Miami, FL, USA

Introduction

Over the past decade, high-rate GPS observations have been used by Larson et al. (2003) and Crowell et al. (2012) to gain increasing information about earthquake-induced strong crustal movements. There are two approaches to process high-rate GPS data: relative positioning and precise point positioning. The two approaches can be considered equivalent in terms of the underlying physics, but precise point positioning has a limitation for GPS seismology, because of unresolved integer-cycle phase ambiguities and slow convergence and reconvergence rates when loss of lock on the satellite signals occurs (Bock et al. 2011). However, the relative positioning approach can also be problematic in the analysis of large magnitude earthquake ($M > 7$), because the earthquake-induced ground motion affects a very large area, including potential reference sites.

The problematic solution of the relative positioning approach became apparent when processing the high-rate (5 Hz) data acquired by the Nicoya Peninsula network right after the 2012, $M = 7.6$ Costa Rica earthquake. All the network stations, which are located within 100 km from the epicenter, were affected by the earthquake. The nearest high-rate station that could be used as a reference site was in Jamaica, more than 1,000 km away and operated with 1 Hz sampling rate. The problem of a moving reference station was less apparent in previous analyses of

Published online: 14 November 2013

high-rate GPS data, because of a lower sampling rate (1 Hz) at the network sites and a reference station available at distances of 300–500 km from the epicenter (Wang et al. 2007).

In this study, we developed a new method based on a spatial filtering technique (Wdowinski et al. 1997) that overcomes the moving reference problem. The method detects the reference station motion, common to all network sites, by using a stacking algorithm and removing the common mode from the time series. We applied the new method to the 2012 Costa Rica earthquake's high-rate GPS data and obtained improved time series of earthquake-induced strong ground movements. The improved time series are free of the reference site motion and also have a lower noise level, because the spatial filtering algorithm also removes systematic common noise from time series of the network.

Methodology

We present here a new post-processing method for improved detection of earthquake-induced ground movements using high-rate GPS data, processed using the relative positioning approach with the GAMIT module TRACK (Herring 2009a, b). The method follows the spatial filtering technique described in Wdowinski et al. (1997), which removes systematic noise common to a number of sites (three or more) in continuous GPS time series of daily positions calculated in a global reference frame. The original spatial filtering technique removed noise associated with orbital errors, weather conditions and other possible causes that can affect in a similar way a number of closely located sites. The current technique is aimed at removing a different noise type, earthquake-induced crustal movements of a near field reference site, which is common to all relative positioning time series in the region after a strong earthquake.

The idea behind the spatial filtering technique is fairly simple and is illustrated in Fig. 1. Earthquake-induced crustal movements are mainly affected by their proximity to the epicenter. Sites located close the epicenter experience high amplitude movements in a relatively short time after the earthquake compared to sites located further away. We illustrate this concept in Fig. 1a, which shows a theoretical time series of four network sites and a near field reference station (RS) located farthest from the epicenter. Because the series are arranged according to their distance to the epicenter, it is easy to see that the signal arrival time increases with the distance from the epicenter, whereas the amplitude decreases with the distance. Using these theoretical time series, we constructed the expected relative positioning time series at the four network sites (Fig. 1b, blue lines). The relative positioning time series are affected by both the network site and the RS, but at different times. The motion of the RS is common to all time series and should be removed from the series.

In order to remove the earthquake-induced movements in the RS from the relative positioning time series, we calculate the common noise or mode (CM) by stacking the time series and dividing the stacked series by the number of series. The first CM time series (CM1 in Fig. 1b) was calculated for the entire time series. It shows that the systematic noise due to the motion in the RS was amplified, whereas the nonsystematic signal in the other network sites, which is the earthquake-induced signal at each network site, was significantly reduced in the CM1 time series. The CM1 series looks somewhat noisy prior to the arrival of the earthquake signal to the RS. However, the noise level decreases with time from the earthquake occurrence, as the amplitude of the earthquake-induced signal decreases with distance from the epicenter. Because the systematic noise begins only after the arrival of the earthquake signal to the RS, we also calculated a shorter CM series (CM2) that begins with the arrival of the

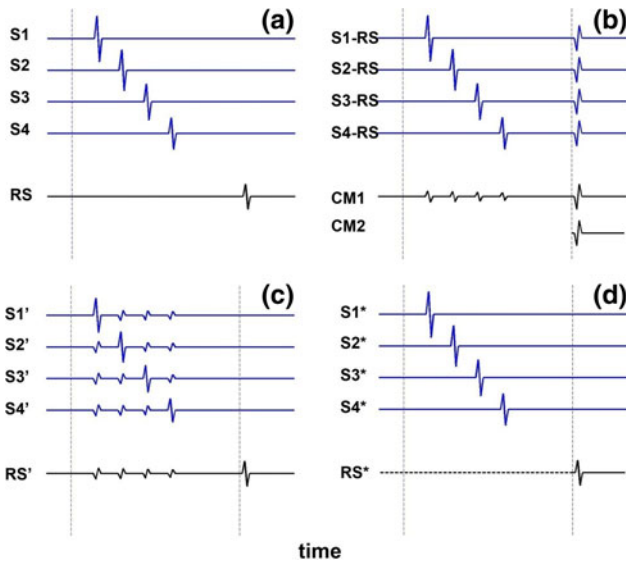

Fig. 1 Schematic illustration explaining the concept of the new spatial filtering technique. **a** High-rate time series of earthquake-induced crustal motion in four network sites (S1, S2, S3 and S4) and the near field reference station (RS). The *vertical dashed line* marks the earthquake's initiation time. **b** The *blues* time series show the relative positioning of the four network sites with respect to the RS. The *black* time series show the common mode of the entire time span (CM1) and of the series since the arrival of the seismic waves to the RS (*black dashed line*) (CM2). **c** Corrected time series obtained by subtracting the common mode (CM1) from the relative positioning time series. The black time series show the negative value of CM1, which represents the motion of the RS. **d** Corrected time series calculated with CM2. The *dashed black horizontal line* presents the assumed null motion of RS prior to the arrival of the earthquake signal

earthquake signal to the RS (vertical black dashed line in Fig. 1b).

After calculating the CM, we can now subtract it from the relative positioning time series and obtain corrected series of the earthquake-induced motion in the network sites that are free of the RS motion. We first calculated the corrected series using common mode of the entire series (CM1). The corrected time series (blue series in Fig. 1c) show the earthquake-induced motion in all the network sites without the RS motion. However, these corrected time series are noisy, due to the propagation of the earthquake-induced signal in the network sites via the CM series. However, when using the shorter CM series that starts with arrival of the earthquake signal to the RS (CM2), the corrected time series are much cleaner (Fig. 1d), because the first part of the time series were not contaminated by the earthquake-induced signal in the network sites as part of the common mode calculations. Instead, we assume a stable behavior of the RS (dashed horizontal black line in Fig. 1d).

We formulated this spatial filtering concept into an algorithm that contains the following three main steps:

Splitting the time series The original displacement series need to be divided into two parts:

$$O^{t}_{\text{raw}}(d) = [\,O^{t1}(d) \quad O^{t2}(d)] \tag{1}$$

Here, O means observation and d means the displacement. Time is in seconds starting at the earthquake rupture: $t1 = 1 \sim m - 1, \quad 0 \le t1 < m; \quad t2 = m \sim t, \quad m \le t2 < t_{\max}$, m is the seismic wave arrival time to the reference site. We can get the time from a known nearby seismometer record, or estimated it from the time difference using epicentral distance and velocity of seismic waves.

Stacking Calculate the common mode of the second part of the time series, epoch-by-epoch, by averaging the values from all S sites

$$\varepsilon(d) = \frac{\sum_{x=1}^{S} \varepsilon_s(d)}{S} \tag{2}$$

$\varepsilon_s(d)$ the relative displacement to the position at the last epoch before the earthquake.

Filtering For of each site, we subtract the reference station movement, which is the common mode, from the $O^{t2}(d)$ part to obtain the filtered displacement series $\hat{O}^{t2}(d)$:

$$\hat{O}^{t2}(d) = O^{t2}(d) - \varepsilon(d) \tag{3}$$

Finally, we combine the two time series:

$$\hat{O}^{t}_{\text{raw}}(d) = [\,O^{t1}(d) \quad \hat{O}^{t2}(d)] \tag{4}$$

The filtered displacement series are given by Eq. (4).

Data and data processing

We tested the new methodology using high-rate GPS data acquired by the Nicoya peninsula GPS network right after the $M = 7.6$ Costa Rica earthquake, which occurred on September 5, 2012 at 14:42:07 UTC. The earthquake ruptured the subduction interface between the subducting Cocos and the overriding Caribbean plates.

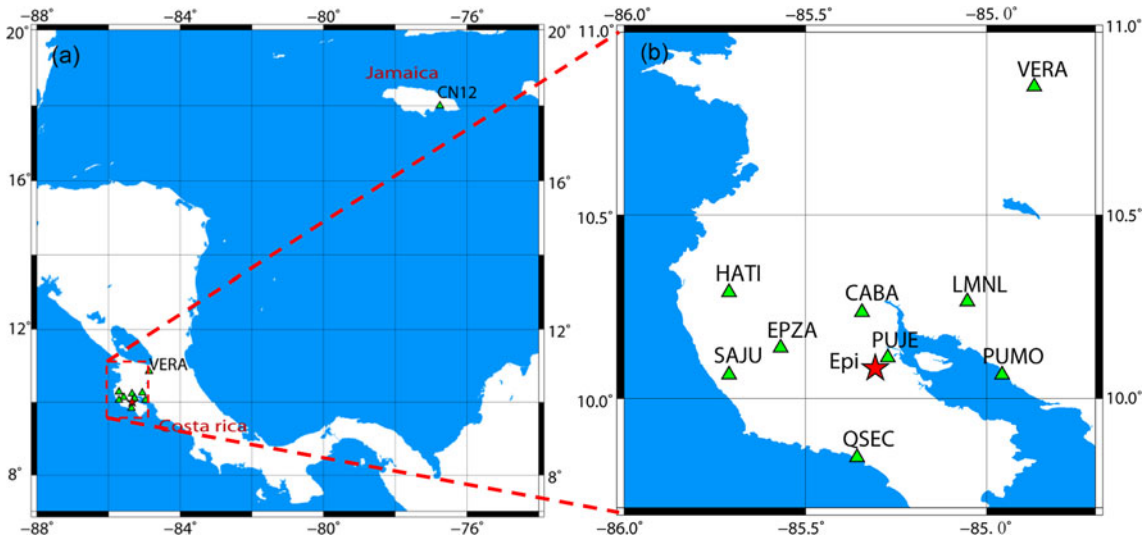

Fig. 2 Geographic locations of stations. *Left* Map of southwestern Caribbean region showing the location of the Nicoya Peninsula, the 2012 $M = 7.6$ earthquake epicenter (*red star*), and the CN12 reference site in Jamaica. *Right* Location map of the high-rate GPS monitoring network in the Nicoya Peninsula with respect to the earthquake's epicenter

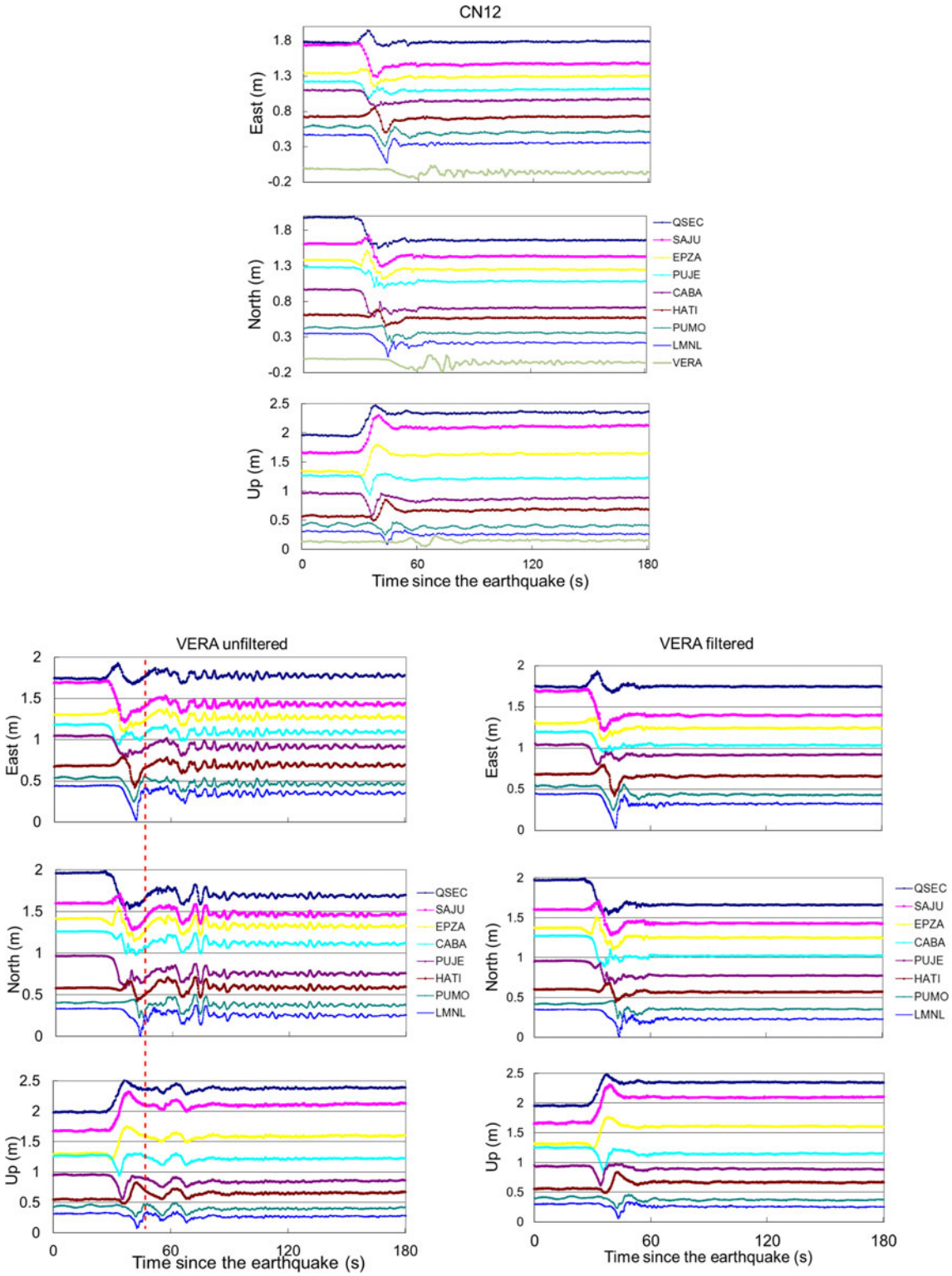

Fig. 3 Displacement time series of the earthquake waveforms, as calculated with respect to CN12 with 1 Hz rate (*top*),with respect to VERA with 5 Hz sampling rate (*left*), and filtered VERA series (*right*). The *red dotted line marks* the arrival time of surface waves to the reference VERA station, 46 s after the event

This study uses data acquired by nine continuous GPS sites installed over the past decade in, or near, the Nicoya Peninsula as part of a GPS network for detecting slow slip events (Outerbridge et al. 2010; Jiang et al. 2012). The nine stations sample at a 5 Hz rate and are located within 100 km from the epicenter (Fig. 2). The

furthest station from the epicenter is VERA, which we chose a reference station in the data analysis.

The high-rate GPS data were processed with the TRACK module (version 1.24) of the GAMIT/GLOBK software package. This module was designed for kinematic GPS data analysis and was successfully used for the study of ice streams (Adalgeirsottir et al. 2008), ocean buoy movements (Schone et al. 2011) and seismic waveforms (Wang et al. 2007; Yin et al. 2010).The data processing requires at least one fixed site, as the software calculates baseline changes in the moving sites with respect to the fixed/reference site. As indicated above, we chose the furthest site from the epicenter, VERA, as the reference site. Because VERA also moved during the earthquake, we introduced a second far field reference site, CN12, which is located in Puerto Rico, more than a 1,000 km away (Fig. 2). We chose this alternative reference site, because it is the nearest high-rate GPS recording site to the Nicoya Peninsula monitoring network. Although it is a high-rate site, its sampling rate is only 1 Hz. In all of our calculations, the data were processed with 15° cutoff elevation mask and IGS final orbits.

Results

Data processing with each of the reference station, VERA and CN12, reveals both advantages and disadvantages. The analysis with the VERA site enables us to calculate waveforms with the full 5 Hz data, but with a large systematic noise resulting from the motion of the VERA site due to the earthquake (Fig. 3, right panel). The systematic noise began 46 s after the earthquake, when surface waves induced by the earthquake reached the VERA site. As a result, all the displacement time series are contaminated by the VERA movements and cannot be used for studying strong ground movements in the other sites.

Processing the data with the CN12 reference site yield an improved displacement time series of the eight sites located in the Nicoya Peninsula representing the actual strong ground motion induced by the earthquake (Fig. 3, left panel). However, these time series are less complete and less accurate than the time series calculated with respect to VERA. Because the CN12 station acquires only 1 Hz data, using it as a reference site also implies that the Nicoya Peninsula network can be determined only with 1 Hz sampling rate. As a result, the time series display only 20 % of the collected data. Another issue that degrades the quality of the CN12 time series is the long distance (>1,000 km) between the reference site and the monitoring network.

We quantified the noise level in each time series using root mean square (RMS) analysis of pre-earthquake data (Table 1).We calculated the RMS of each component, for all time series, using 1,000 s data prior to the earthquake. We chose 1,000 s as a reference data segment, because it is significantly longer than the 180 s segment of the earthquake-induced strong ground movements (Fig. 3). Calculations of shorter segments similar in length to the strong crustal movement record yielded similar RMS results. We chose to use the data just prior to the earthquake, because of similar atmospheric conditions and satellite configuration to those occurring during and after the earthquake. Comparison between RMS values calculated with VERA and CN12 reference sites shows a much lower noise level in the VERA RS time series (Table 1). The VERA-based RMS results are 1.2–3 times lower than those calculated with the CN12 reference site. These results likely reflect the large differential atmospheric conditions between the CN12 site in Jamaica and network sites in western Costa Rica.

Improved time series

We used our spatial filtering algorithm (see "Methodology") in order to improve the signal in the near field time series that uses the site VERA as RS. The algorithm includes three steps: splitting the series, stacking and filtering. The first step is splitting the series into pre- and post-arrival of the seismic waves to the RS. The series waveforms show a transition 46 s after the earthquake (Fig. 3, vertical red line), representing the arrival time of the seismic wave to the RS. Before this transition, each time series exhibits a different behavior. However, after

Table 1 GPS station locations and RMS noise estimation of the three displacement components

Station name	Longitude (°W)	Latitude (°N)	RMS (VERA/CN12)		
			East (mm)	North (mm)	Up (mm)
CN12	76.750	18.000	–	–	–
VERA	84.869	10.853	–	–	–
QSEC	85.357	9.840	3.6/7.3	2.2/2.7	4.3/6.5
SAJU	85.710	10.067	2.9/6.1	1.6/2.6	6.1/10.1
EPZA	85.568	10.140	4.3/6.5	2.8/3.8	5.9/6.6
CABA	85.343	10.237	2.7/7.8	1.8/2.2	4.7/6.3
PUJE	85.272	10.113	2.4/5.5	1.6/2.3	5.2/7.3
HATI	85.710	10.292	4.7/6.1	1.5/3.9	4.6/10.3
PUMO	84.966	10.064	2.3/9.1	1.7/3.6	3.3/9.5
LMNL	85.053	10.267	2.8/5.2	2.2/4.7	3.2/7.3

CN12 and VERA are both used as reference stations, and hence, no time series were calculated for them. The RMS (VERA/CN12) means the left/right value is obtained with respect to VERA/CN12 references stations

46 s, all series show very similar oscillatory patterns reflecting the contribution of the RS's earthquake-induced movements to the relative positioning time series. Thus, we split the series at 46 s after the earthquake.

The second and third steps of the algorithm consist of stacking and filtering the second part of the time series. We followed these steps using (2) and (3) and obtained improved time series, free of the oscillatory movement of the RS (Fig. 3, right panel). The improved series have a very similar shape as the series calculated with the far field station CN12 (Fig. 3, left panel). We conducted a systematic comparison between the two calculations by plotting the two series together (Fig. 4). The comparison shows a very good fit between the two calculations. The overall shape of the waveform is basically identical when using the far field and improved near field reference sites. However, the improved near field series, calculated with 5 Hz sampling rate, contains significantly more information, five

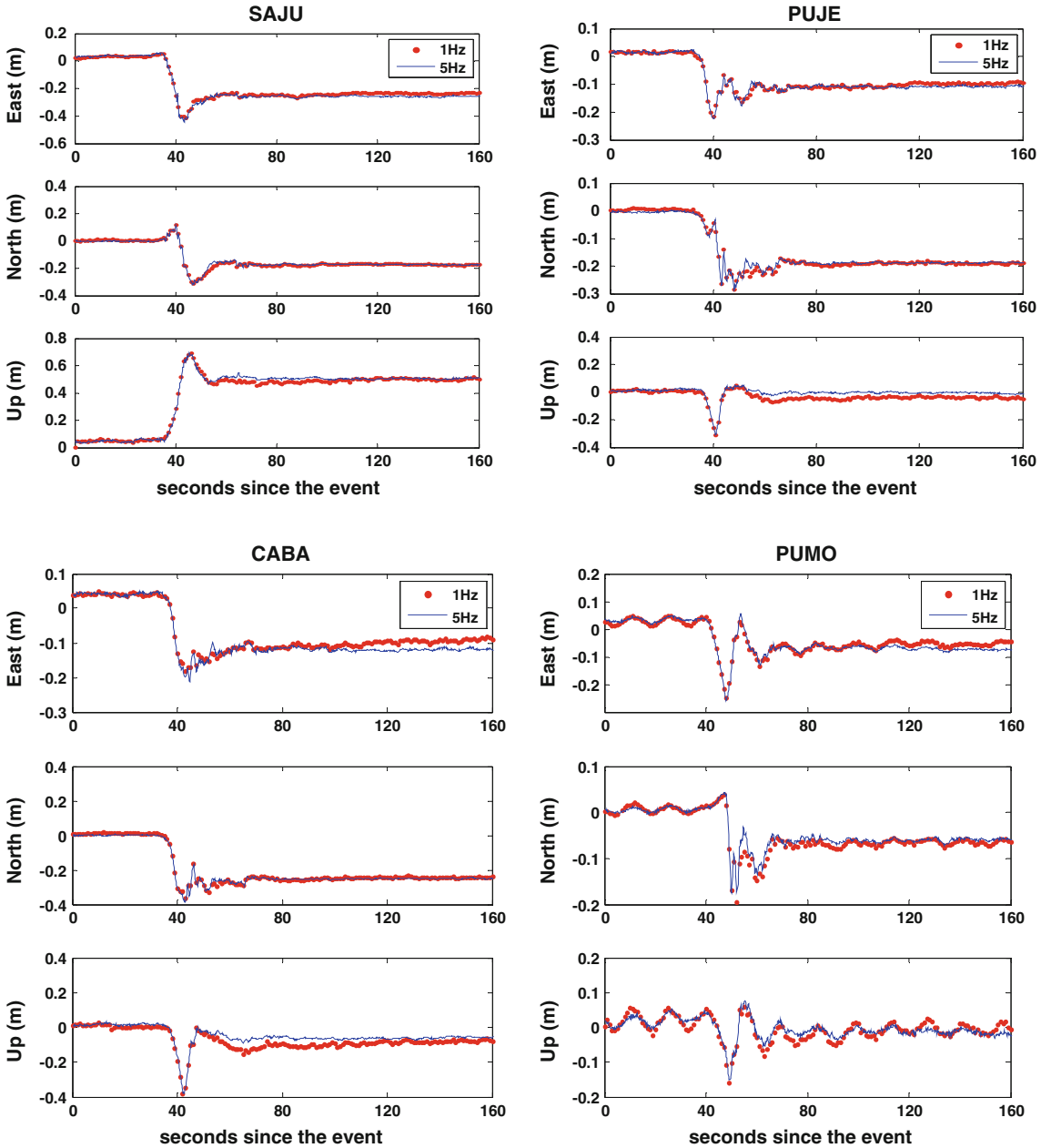

Fig. 4 Examples of misfit between the improved near field, 5 Hz time filtered series (VERA as the reference station, *blue lines*) and the far field 1 Hz raw series (CN12 as the reference station, *red dots*). The RMS values represent the misfit level between the two series. For SAJU: $RMS_E = 13.2$ mm, $RMS_N = 8.3$ mm and $RMS_U = 17.7$ mm; For PUJE: $RMS_E = 8.3$ mm, $RMS_N = 8.5$ mm and $RMS_U = 18.1$ mm. For CABA: $RMS_E = 12.6$ mm, $RMS_N = 8.4$ mm and $RMS_U = 18.5$ mm; For PUMO: $RMS_E = 13.0$ mm, $RMS_N = 8.8$ mm and $RMS_U = 15.2$ mm

times as much. Furthermore, a careful inspection of the two series shows some misfit between the two series. We quantified the misfit between the two series using RMS analysis, which indicates a misfit level of 8–17 mm (Fig. 4). This misfit level is higher than the RMS difference between the two series prior to the earthquake (Table 1) reflecting both large differential atmospheric condition in the long baseline solutions and drifting solutions (CABA east in Fig. 4), which often occurs in long baseline (>500 km) solutions.

Conclusions

We developed a new method for improving high-rate GPS time series of earthquake-induced ground movements calculated with a relative positioning method, based on the TRACK module of GAMIT. The method uses a near field reference site and, hence, yields more accurate short baselines solutions, compared to the traditional use of far field reference site. Although the near field site moved by the earthquake, which affected all the time series, we were able to remove those movements of the reference site from the series using a modified version of the spatial filtering technique. The improved time series provides a better measure of earthquake-induced crustal movements than those calculated with a far field site.

We applied the new method to data collected by the Nicoya Peninsula high-rate GPS network, which recorded near field ground movements induced by the 2012, $M = 7.6$ Costa Rica Earthquake in nine stations. This high-rate record is a unique dataset, as the stations recorded in 5 Hz sampling rate and the earthquake occurred at the center of the network. We processed these data with the TRACK module of GAMIT using both a near field and a far field reference sites. The nearest far field high-rate reference site was in Jamaica, more than 1,000 km from the earthquake epicenter, and operated at 1 Hz. Using this reference site degraded the accuracy and temporal resolution of the solution. However, by using the new spatial filtering method, we were able to calculate the earthquake-induced movements at a 5 Hz rate and with improved accuracy due to the shorter baseline. A comparison of the filtered time series with the far filed reference site series shows a very good agreement between in the overall shape the two time series, indicating that the new spatial filtering method is accurate. Furthermore, the method produces solutions at the maximum sampling rate of 5 Hz, which cannot be obtained by the far field reference site analysis. The spatial filtering method also removes other systematic common noise from the time series, possibly due to atmospheric delay or orbital errors and, hence, produces more accurate solutions that are based on far fields sites.

Acknowledgments We acknowledge UNAVCO as the source of the high-rate GPS data. We thank Professor Thomas Herring for his patient guidance in operating his kinematic GPS data processing program "TRACK" module of GAMIT/GLOBK. This work was supported by National Technology Support Project (2012BAK19B04), the National Natural Science Foundation of China (41104023), China Scholarship Council.

References

Adalgeirsottir G, Smith AM, Murray T, King MA, Makinson K, Nicholls KM, Behar AE (2008) Tidal influence on Rutford Ice stream, West Antarctica: observations of surface flow and basal processes from closely spaced GPS and passive seismic stations. J Glaciol 54(187):715–724

Bock Y, Melgar D, Crowell BW (2011) Real-time strong-motion broadband displacements from collocated GPS and accelerometers. Bull Seismol Soc Am 101:2904–2925. doi:10.1785/0120110007

Crowell BW, Bock Y, Melgar D (2012) Real-time inversion of GPS data for finite fault modeling and rapid hazard assessment. Geophys Res Lett 39:L09305. doi:10.1029/2012GL051318

Herring TA (2009b) TRACK GPS kinematic positioning program, version 1.21. Massachusetts Institute of Technology, Cambridge

Herring TA (2009c) Example of the usage of TRACK. Massachusetts Institute of Technology, Cambridge. http://geoweb.mit.edu/_tah/track_example/

Jiang Y, Wdowinski S, Dixon TH, Hackl M, Protti M, Gonzalez V (2012) Slow slip events in Costa Rica detected by continuous GPS observations, 2002–2011. Geochem Geophys Geosyst 13:Q04006. doi:10.1029/2012GC004058

Larson K, Bodin P, Gomsberg J (2003) Using 1 Hz GPS data to measure deformations caused by the Denali fault earthquake. Science 300:1421–1424

Outerbridge KC, Dixon TH, Schwartz SY, Walter JI, Protti M, Gonzalez V, Biggs J, Thorwart M, Rabbel W (2010) A tremor and slip event on the Cocos-Caribbean subduction zone as measured by a GPS and seismic network on the Nicoya Peninsula, Costa Rica. J Geophys Res 115(B10):B10408. doi:10.1029/2009jb006845

Schone T, Pandoc W, Mudita I, Roemer S, Illigner J, Zech C, Galas R (2011) GPS water level measurements for Indonesia's Tsunami Early Warning System. Nat Hazards Earth Syst Sci 741–749. doi:10.5194/nhess-11-741-2011

Wang G, Boore DM, Tang G, Zhou X (2007) Comparisons of ground motions from collocated, closely spaced one-sample-per-second Global Positioning System, accelerograph recordings of the 2003 M 6.5 San Simeon, California, earthquake in the Parkfield Region. Bull Seismol Soc Am 97(1B):76–90

Wdowinski S, Bock Y, Zhang J et al (1997) Southern California permanent GPS geodetic array: spatial filtering of daily positions for estimating coseismic and postseismic displacements induced by the 1992 Landers earthquake. J Geophys Res 102:18057–18070

Yin HT, Zhang PZ, Gan WJ, Wang M, Liao H, Li XJ, Li J, Xiao GR (2010) Near-field surface movement during the Wenchuan Ms8.0 earthquake measured by high-rate GPS. Chin Sci Bull 55. doi:10.1007/s11434-010-4026-2

Author Biographies

Dr. Haitao Yin is an associate researcher at the Earthquake Administration of Shandong Province, China. His work has focused

on the high-rate GPS data processing and strong ground movement analyzing. He successfully obtained the co-seismic crustal deformation of 2008 Ms8.0 Wenchuan Earthquake.

Dr. Shimon Wdowinski is a research associate professor at the Rosenstiel School of Marine and Atmospheric Sciences, University of Miami, where he teaches and researches geology and geophysics. His work has focused on the development and usage of space geodetic techniques that can detect very precisely small movements of the earth's surface.